

New Additions to the *Paranthropus boisei* Mandibular Hypodigm from Koobi Fora, Kenya

LUCÍA NADAL*

Leverhulme Centre for Human Evolutionary Studies, Department of Archaeology, University of Cambridge, Cambridge, UNITED KINGDOM; and, Turkana Basin Institute, Nairobi, KENYA; ln340@cam.ac.uk

LOUISE LEAKEY

Turkana Basin Institute, Nairobi, KENYA; and, Department of Anthropology, Stony Brook University, Stony Brook, USA; louise.leakey@stonybrook.edu

MEAVE LEAKEY

Turkana Basin Institute, Nairobi, KENYA; and, Department of Anthropology, Stony Brook University, Stony Brook, USA; meave.leakey@stonybrook.edu

MARTA MIRAZÓN LAHR

Leverhulme Centre for Human Evolutionary Studies, Department of Archaeology, University of Cambridge, Cambridge, UNITED KINGDOM; and, Turkana Basin Institute, Nairobi, KENYA; mbml1@cam.ac.uk

corresponding author: Lucía Nadal; ln340@cam.ac.uk

submitted: 21 May 2023; revised: 3 September 2023; revised: 17 September 2023; revised: 20 December 2023; accepted: 29 December 2023

Handling Editor in Chief: Katerina Harvati

ABSTRACT

After teeth, mandibles and mandibular fragments are the best represented element in the early hominin fossil record. Among these, the mandibular hypodigm of *Paranthropus boisei* stands out as one of the largest ascribed to a single early hominin species, comprising 39 published fossil specimens. Fossils of *P. boisei* originate from eight localities spread over 1,800km in a North-South axis across eastern Africa—from the site of Malema in Malawi to that of Konso in Ethiopia. However, the vast majority of the remains originate from Koobi Fora in northern Kenya. Most of the Koobi Fora hominins were discovered during the first decade of exploration of the site (1969–1979), and (besides those singularly important fossils that were published in scientific journals) were described in a major monograph by B. Wood in 1991. Some of the fossils discovered since have yet to be described and analyzed. Here, we describe two previously unpublished hominin mandibles, KNM-ER 42709 and KNM-ER 42801, found by the Koobi Fora Research Project led by Meave and Louise Leakey. Both fossils show mandibular and dental dimensions, as well as autapomorphic traits, typical of *P. boisei*. We explore quantitatively the position of these two fossils within the diversity of *P. boisei* mandibles and discuss their implications for the evolutionary history of the species.

INTRODUCTION

The spatial and temporal ranges of *Paranthropus boisei* are some of the most extensive among early hominin species. Spatially, fossils ascribed to the species originate in eight localities in four East African countries—Malema in Malawi, Olduvai Gorge and Peninj in Tanzania, West Turkana, Koobi Fora, and Chesowanja in Kenya, and Omo Shungura and Konso in Ethiopia—spanning a geographical range of 1,800km N-S (Wood and Constantino 2007). Chronologically, the species has a duration of approximately one million years, with the earliest fossils from Omo Shungura at ca. 2.3 Ma (Kullmer et al. 1999), and the most

recent from Olduvai Gorge at 1.34 Ma (Dominguez-Rodriguez et al. 2013).

Despite these wide temporal and geographical ranges, there is a general consensus that the species is relatively homogenous, lacking clear temporal (Wood et al. 1994) or paleoenvironmental (White 1988) trends. Another intriguing aspect of *P. boisei* is its disappearance from the fossil record after 1.3 Ma, for which there are currently two main hypotheses. One attributes its extinction to ecological competition with early *Homo* (e.g., Klein 1988) with whom *P. boisei* is known to have lived sympatrically (Leakey and Leakey 1964; Leakey and Walker 1976); the other, to the

taxon's C_4 plant dietary specialization that may have limited its capacity to adapt to changes in the availability of C_4 resources (e.g., Wood and Patterson 2020; Wood and Strait 2004). Neither hypothesis is without criticism. *P. boisei* and early *Homo* coexisted for hundreds of thousands of years, so had likely established some form of long-term niche partitioning. Furthermore, the alleged drastic change in paleovegetation distribution that would have made C_4 resources unavailable remains highly contested (Patterson et al. 2017; 2022; Quinn and Lepre 2021; Quinn et al. 2013). The notion that *P. boisei*'s highly derived morphology might not preclude a more generalist diet (Ungar et al. 2008) compounds the issue further. In this context, the scarcity of *P. boisei* fossils dated to the last hundred thousand years of the species' known temporal range, between 1.45 and 1.34 Ma, has significantly impeded answering questions about the roles of diet and competition prior to the species extinction. This makes any addition to the species hypodigm from this period particularly important.

After isolated teeth, more than half of the *P. boisei* hypodigm consists of fossil mandibles (39 mandibular specimens, 55% of the non-dental hypodigm), the vast majority of which derive from Koobi Fora in the eastern shore of Lake Turkana, Kenya (30 mandibles, ~76%). From a historical standpoint, Koobi Fora is notable for being one of the most prolific fossil localities in Africa (Harris et al. 2006). The Koobi Fora Research Project (KFPR), founded by Richard and Meave Leakey in 1975, has since then undertaken yearly fieldwork seasons and continues to contribute new and significant discoveries to the existing hominin fossil record (e.g., Leakey et al. 2012; Spoor et al. 2007). Contextualizing these new fossil specimens within a taxonomic framework remains a crucial first step for their interpretation. Furthermore, the intraspecific implications that new discoveries might have for the interpretation of extinct hominin species are fundamental to expanding our analytical resolution of the evolutionary history of individual taxa.

Because of its rich fossil record, *P. boisei* offers a unique opportunity to explore intraspecific variability in extinct hominins. The addition of new fossil specimens to the species hypodigm not only increases our understanding of this intraspecific variability, but it also increases the temporal, geographical, and ecological framework within which to interpret it. Here, we describe and comparatively analyze two unpublished mandibular fossils from Koobi Fora, informally attributed to *P. boisei* at the time of discovery—KNM-ER 42709 and KNM-ER 42801. We confirm this taxonomic attribution, quantitatively assess their placing within the taxon's variability, and discuss the implications for our understanding of the species diversity in time and space. KNM-ER 42709 (Figure 1A, B, C, and D) is a left edentulous mandibular corpus with roots of M_3 to I_1 present. It derives from a stratigraphic context within area 6A consistent with an age of ca. 1.4 million years (Ma), making this the last currently known appearance of *P. boisei* in Kenya. KNM-ER 42801 (Figure 1E, F, G, H, and I) is a small fragment of mandibular corpus with the crown of the M_3 present. Its stratigraphic context within area 8B suggest a date of ca. 1.55 Ma.

METHODS

GEOLOGICAL CONTEXT AND DATING

We reconstructed the sedimentological context of the specimens presented here from field records and original field slips of the KFPR kept at the National Museums of Kenya in Nairobi. We used GPS coordinates taken upon collection using a Garmin GPS handheld device to locate the fossils within the Koobi Fora collection areas and correlated the original notes with the stratigraphic columns described for the pertinent collection areas by Gathogo and Brown (2006) to reconstruct their geological context. Geological age estimates are based on these stratigraphic placements.

GENERAL DESCRIPTIONS AND MEASUREMENTS

KNM-ER 42709 and KNM-ER 42801 are both housed at the National Museums of Kenya in Nairobi, where detailed anatomical descriptions were made for each specimen. Standard mandibular and dental measurements were taken with a digital caliper and rounded to the nearest 0.01mm. Additionally, high-resolution 3D surface scans were obtained using an Artec Space Spider scanner. Mandibular and dental measurements for each specimen can be found in the Supplementary Materials Table S1.

COMPARATIVE METRIC ASSESSMENT AND TAXONOMIC ATTRIBUTION

A comparative dataset of eight measurements of the mandibular corpus and M_3 crown of a large fossil hominin sample was compiled from the data presented by Wood (1991a). The choice of measurements was restricted to those that could be taken on the new fossils being described, namely mandibular height and width at M_1 , M_2 , and M_3 , and M_3 mesiodistal and buccolingual diameters. The comparative sample includes adult specimens attributed to *Australopithecus africanus*, *Australopithecus afarensis*, *Homo habilis*, *Homo erectus*, *Paranthropus aethiopicus*, *Paranthropus robustus*, and *P. boisei*, and are listed individually in Supplementary Materials Tables S1–5. Inter-observer error was assessed by evaluating the differences in corpus height and width at M_1 in five fossil specimens (KNM-ER 1468, KNM-ER1469, KNM-ER725, KNM-ER 729, and KNM-ER 403) taken by one of the authors (LN) and those in Wood (1991a), and comparing them to the differences found between specimens. A Student's t-test revealed the inter-observer error to be significantly lower than the intra-sample variability for both the height ($t = -3.53$, $p\text{-value} = 0.0038$) and the width ($t = -3.32$, $p\text{-value} = 0.0072$) at M_1 , therefore having a negligible impact on the analysis. Furthermore, intra-observer error was evaluated by comparing the differences obtained from three repetitive measurements of KNM-ER 42709 of corpus height and width at M_2 , to the differences observed between this reference specimen and KNM-ER 42801. A Student's t-test shows the intra-observer error to be lower than the variation between samples for height ($t = -355.3$, $p\text{-value} = 7.96 \times 10^{-6}$) and width ($t = -9.46$, $p\text{-value} = 0.0109$).

In order to assess the presence of taxonomically diag-

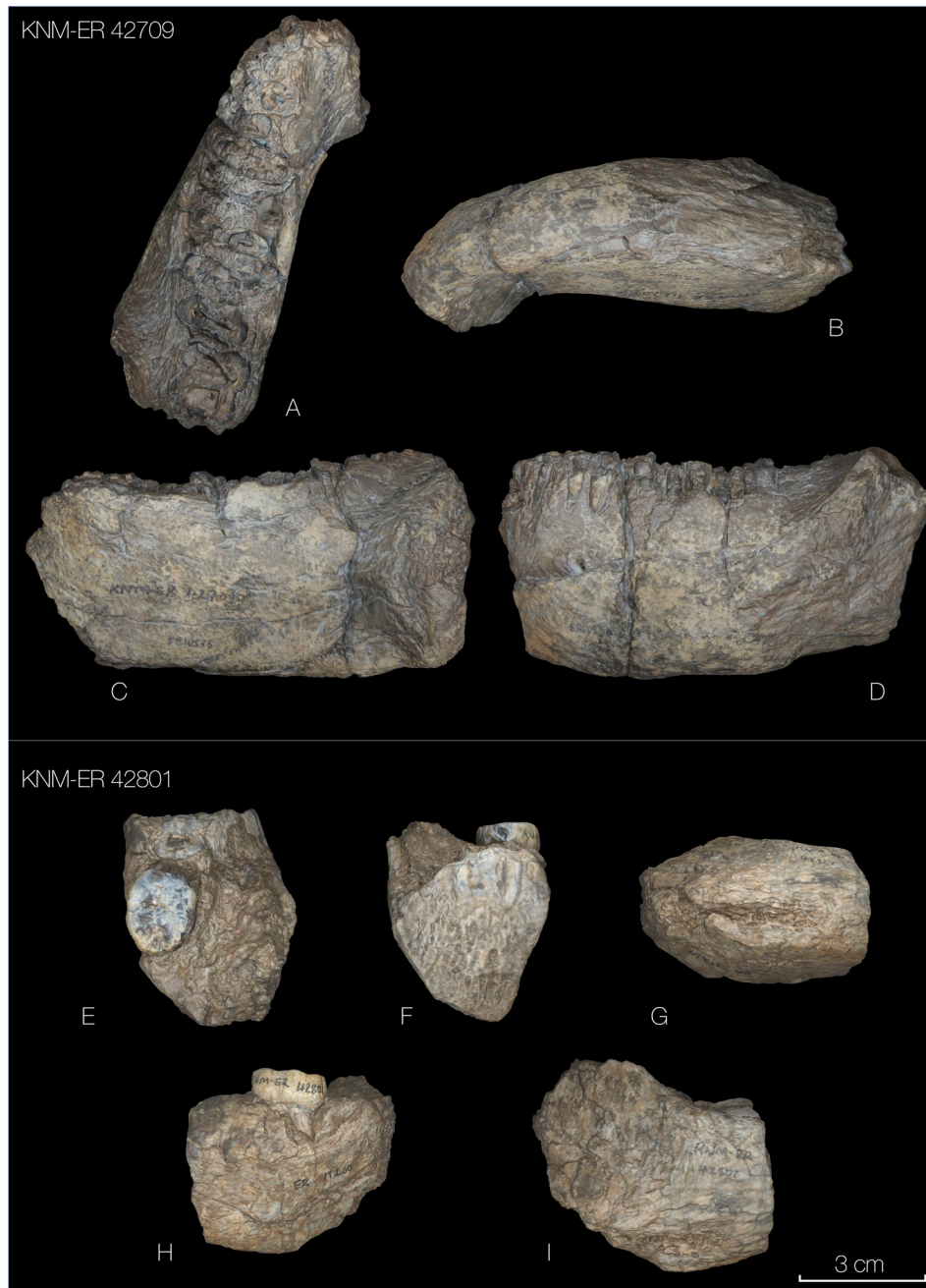


Figure 1. KNM-ER 42709 in dorsal (A); ventral (B); right lateral (C); and left lateral (D) views; and KNM-ER 42801 in dorsal (E); posterior (F); ventral (G); left lateral (H) and right lateral (I) views.

nostic features in KNM-ER 42709 and KNM-ER 42801, the character state of 3 mandibular and 3 dental morphological features was observed by two of the authors (LN, MML). The selection of these traits was constrained by the preservation of the specimens being described and includes the presence and configuration of inferior and superior transverse tori, the extent and position of the lateral corpus prominence, the extent of the extramolar sulcus, the premolar root morphology, and the presence/absence of lingual and distal M_3 accessory cusps. More information on these features and their character state in *P. boisei* and

other hominins can be found in Supplementary Materials Table S6.

GEOMETRIC MORPHOMETRIC AFFINITIES

Geometric morphometric methods (GMM) were used to evaluate the placement of the fossils described in this study within the *P. boisei* mandibular hypodigm. This landmark-based analytical approach represents an alternative to linear measurements for the quantification and statistical analysis of shape and uses Cartesian coordinate data from designated anatomical landmarks that share homol-

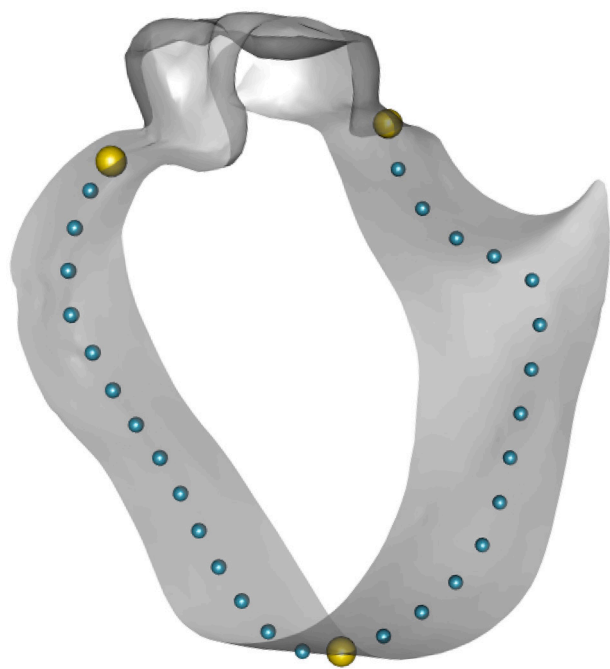


Figure 2. Landmark design used for geometric morphometric comparisons of KNM-ER 42709 and KNM-ER 42801. Fixed landmarks are shown in yellow and curve semi-landmarks in blue. See Table 1 for landmark placement definitions.

ogy across specimens (for more comprehensive reviews on GMM see Bookstein 1991; Gunz and Mitternrocker 2013; Klingenberg 2010). The 3D landmark design used for analyzing the two new fossil specimens was constrained by the state of preservation of KNM-ER 42801. This landmark template consisted of 3 fixed landmarks and 28 curve semi-landmarks encircling the mandibular corpus at medial M_2 (Figure 2). Fixed landmarks were placed by a single observer (LN) and intra-observer error was assessed by landmarking a single sample (KNM-ER 42709) ten times. The mean Procrustes distance obtained was then compared to the distances between this reference sample and the remaining samples included in the geometric morphometric analysis. A Student's t-test shows that the intra-observer error is significantly lower than variation observed between

samples ($t=3.294$, $p\text{-value}=0.0034$) and therefore does not have a significant effect on landmark placement. Fixed and curve semi-landmark definitions for this design are described in Table 1.

The GMM analyses entailed landmark patching, sliding by minimizing bending energy, and Procrustes superimposition, which were done in the Morpho package in R (v2.9; Schlager 2017). Principal component analyses of the landmark design dataset and plotting of backtransform morphospaces using thin-plate spline deformations were used to interpret the morphological affinities of KNM-ER 42709 and KNM-42801.

RESULTS

GEOLOGICAL CONTEXT AND DATING

KNM-ER 42709

This specimen was found by Justus Erus Edung, a member of the KFPR team during the 2002 field season, in collection Area 6A (4.293860 °N, 36.245870 °E), west of the current Ileret field station of the Turkana Basin Institute. The stratigraphic section on Area 6A (PNG-06A) by Gathogo and Brown (2006), taken approximately 1000 meters southeast of the discovery site, was used to reconstruct the sedimentological context of KNM-ER 42709 (Figure 3B). KNM-ER 42709 was found on the surface, deriving from a claystone bed that underlies the pink dolomite layer, a distinct marker of the Upper Okote Member in the area near Ileret (Brown and Feibel 1986; Gathogo and Brown 2006). The Okote member in the Ileret area is delimited by the Ileret Tuff Complex underneath and the Chari Tuff above, with $^{40}\text{Ar}/^{39}\text{Ar}$ radiometric dating yielding a geochronological range between 1.38 and 1.56 Ma (Brown et al. 2006; McDougall and Brown 2006). KNM-ER 42709 derives from the upper section of a sequence of claystones and siltstones called 'the main fish bed', which underlies the pink dolomite, and is also considered a key marker of the Upper Okote Member in the Ileret area (Figure 3C). This 'main fish bed' has been estimated to have an age of 1.42 Ma (Gathogo and Brown 2006; Spoor et al. 2007), constraining the age of KNM-ER 42709 to between 1.38 and 1.42 Ma, with an average age of 1.40 Ma.

TABLE 1. LANDMARK DEFINITIONS.

No.	Name	Definition
1	Medial lingual M_2	Midpoint at M_2 on lingual alveolar face
2	Corpus base at M_2	Most inferior point on corpus base at medial M_2
3	Medial buccal M_2	Midpoint at M_2 on buccal alveolar face
4–17	Lingual corpus face	A curve along the lingual face of the mandibular corpus, beginning at 1 and ending at 2.
18–31	Buccal corpus face	A curve along the buccal face of the mandibular corpus, beginning at 2 and ending at 3

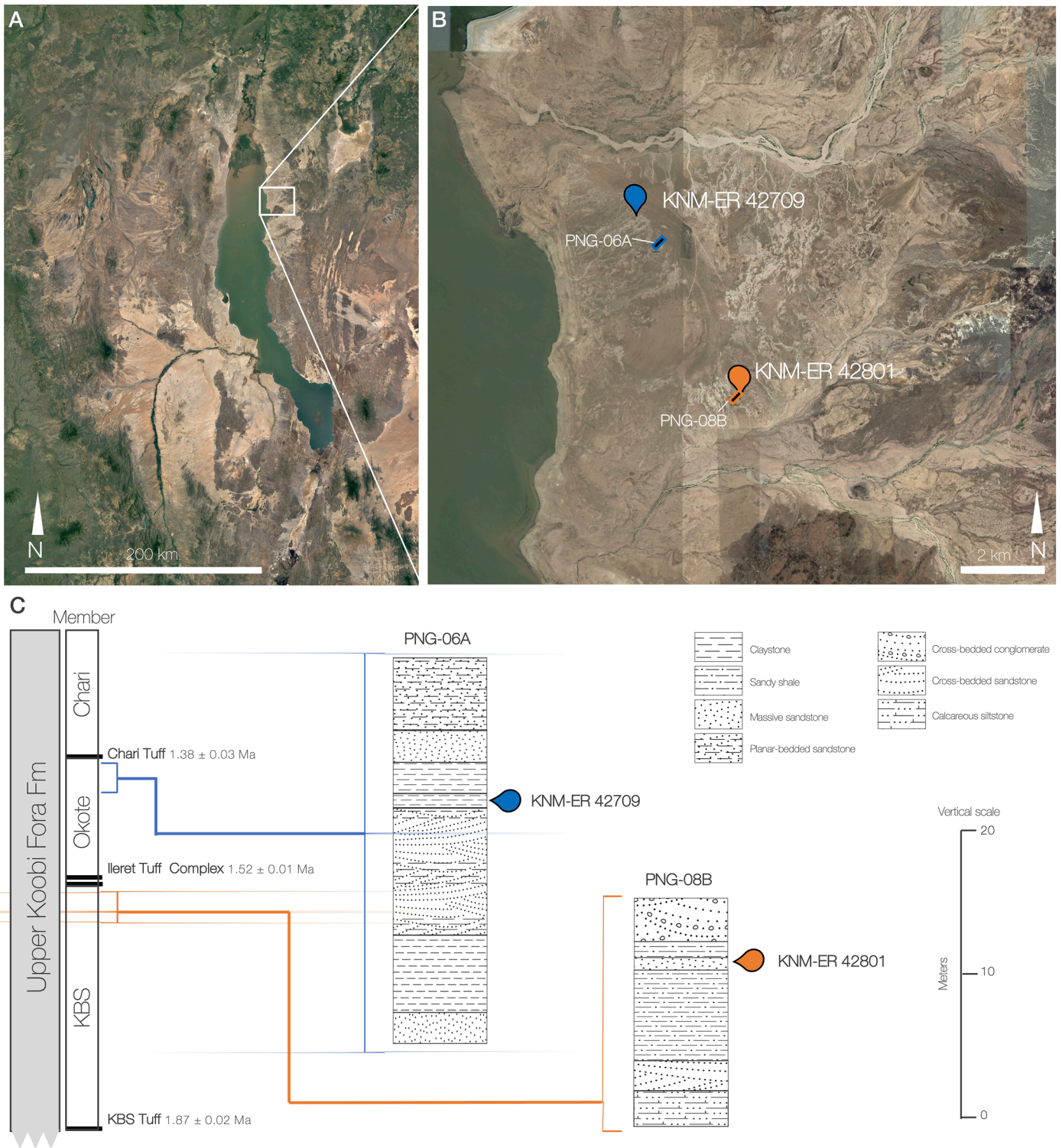


Figure 3. Geographical context within the Turkana Basin (A) of KNM-ER 42709 and KNM-ER 42801 and the location of stratigraphic sections PNG-06A and PNG-08B from Gathogo and Brown (2006) (B). Stratigraphic columns for sections PNG-06A and PNG-08B are shown within the context of the Upper Koobi Fora Formation and its main tuffs, and the stratigraphic context of KNM-ER 42709 and KNM-ER42801 is marked.

KNM-ER 42801

This specimen was discovered by Sila Dominic in Area 8B (4.239097°N, 36.276936°E), also during the KFRP 2002 field season. The stratigraphic section by Gathogo and Brown (2006) of Area 8B (PNG-08B) used to reconstruct the stratigraphic context of the find was taken 60 meters northwest of the discovery site. KNM-ER 42801 was found on the surface, originating from siltstone strata found above the major sandstone of the Upper KBS Member (see Figure 3B and C). The KBS Member is geochronologically well-defined by the Ileret Tuff Complex at the top (1.56 Ma) and the KBS Tuff underneath (1.86 Ma), and the major sandstone is a well-known marker of the upper section of the KBS member in the Ileret Area. Assuming constant sedimentation rates, this major sandstone bed has been estimated to have an age of 1.55 ± 0.01 Ma by Spoor et al. (2007), making it the age estimate for KNM-ER 42801.

DESCRIPTIONS**KNM-ER 42709**

KNM-ER 42709 is a left mandibular corpus fragment with roots of the M_3 to the I_1 , and no crowns present (see Figure 1A, B, C, and D). The specimen is fractured anteriorly at the symphysis in a vertical plane and posteriorly distal to the M_3 alveolus. Anteriorly, a fracture runs vertically through the roots of the P_4 , showing two fragments that have been glued together in the past. Matrix filled cracks are not observed; however, evidence of erosion can be appreciated on all surfaces. Furthermore, a layer of the buccal surface of the corpus from the distal M_1 to M_3 , as well as the superior portion of the buccal symphyseal surface, is missing.

Lingual morphology of the symphysis and corpus. The lingual aspect of the symphysis is characterized by a large inferior and a relatively smaller superior torus separated by an extremely shallow glenoglossal fossa, so that both tori form a single large buttress. The digastric and the submandibular fossae are extremely shallow.

Buccal morphology of the symphysis and corpus. The anterior fracture prevents a clear observation of what could be a mental protuberance. There is a prominence on the base of the corpus at the level of the P_4 . The mental foramen lies at the level of the distal root of the P_3 , and has a diameter of 3.35mm. There is a lateral prominence at the level of the M_1 - M_2 , just below the origin of the oblique line. What remains of the extramolar sulcus is shallow.

Dentition. Only the roots of the M_3 to I_2 are preserved *in situ*. The exposed root sections of the P_3 and P_4 display two flattened dish-shaped mesiodistal roots, with each root showing two root canals positioned buccolingually. The lingual section of the very large proximal root of M_1 is missing.

KNM-ER 42801

KNM-ER 42801 is a small, robust fragment of right mandibular corpus that preserves the crown of the M_3 (see Figure 1E, F, G, H, and I). The coronal plane of the anterior

fracture runs perpendicular to the base through the mesial root of the M_2 ; the posterior fracture surface runs through the oblique line and the anterior aspect of the ramus. A portion of the corpus base at the level of the M_3 is heavily eroded, although no matrix filled cracks are present. The extramolar sulcus still has matrix attached.

Lingual morphology of the symphysis and corpus. While little of the lingual aspect of the corpus remains, the beginning of a submandibular fossa can be observed.

Buccal morphology of the symphysis and corpus. The buccal aspect of the corpus displays a lateral prominence at the level of the M_2 - M_3 . What remains of the base of the corpus displays a well-defined sharp inferior angle.

Dentition. The M_3 crown shows no dentine exposure; however, all cusps are significantly worn. What remains of the fissures suggests a contact between the metaconid and the hypoconid, forming an 'X' pattern. Three accessory C6 cusps (tuberculum sextum) are observed on the distal aspect between the hypoconulid and the entoconid. There is no evidence of a C7 cusp (tuberculum intermedium) or a protostylid.

COMPARATIVE METRIC ASSESSMENT AND TAXONOMIC ATTRIBUTION**KNM-ER 42709**

Metric comparisons of corpus width and height at M_1 , M_2 , and M_3 show that KNM-ER 42709 falls within the range of variation of *P. boisei* (Figure 4). Moreover, KNM-ER 42709 displays the mesiodistal arrangement, or 'molarized' condition, of the two roots of both the P_3 and P_4 , which represents one of the most characteristic traits of *P. boisei* (Wood et al. 1988). The preserved corpus morphology further displays several other affinities with *P. boisei*. These include the presence of large superior and inferior transverse tori on the lingual aspect of the corpus and of a substantial lateral prominence on the buccal aspect of the mandible, traits considered diagnostic of this species (Wood and Constantino 2007). Affinities with early *Homo* are rejected based on KNM-ER 42709's overall size and robusticity, and 'molarized' premolar roots (Wood et al. 1988), despite the overlap in geographical and temporal ranges.

KNM-ER 42801

As with KNM-ER 42709, the dimensions of KNM-ER 42801 fall within the range of variation of *P. boisei* in corpus width and height at M_2 and M_3 (see Figure 4B and C). While little of the corpus morphology is preserved, the substantial lateral prominence and wide extramolar sulcus corroborate the affinities of KNM-ER 42801 with *P. boisei*. The mesiodistal and buccolingual dimensions of the M_3 crown are within the range of *P. boisei* (Figure 5), while the presence of three C6 accessory cusps are also diagnostic of *P. boisei* (Wood and Abbott 1983), further confirming the attribution of KNM-ER 42801 to this species. Additional dental traits that support this attribution include the absence of both a protostylid and a tuberculum intermedium (i.e., C7 acces-

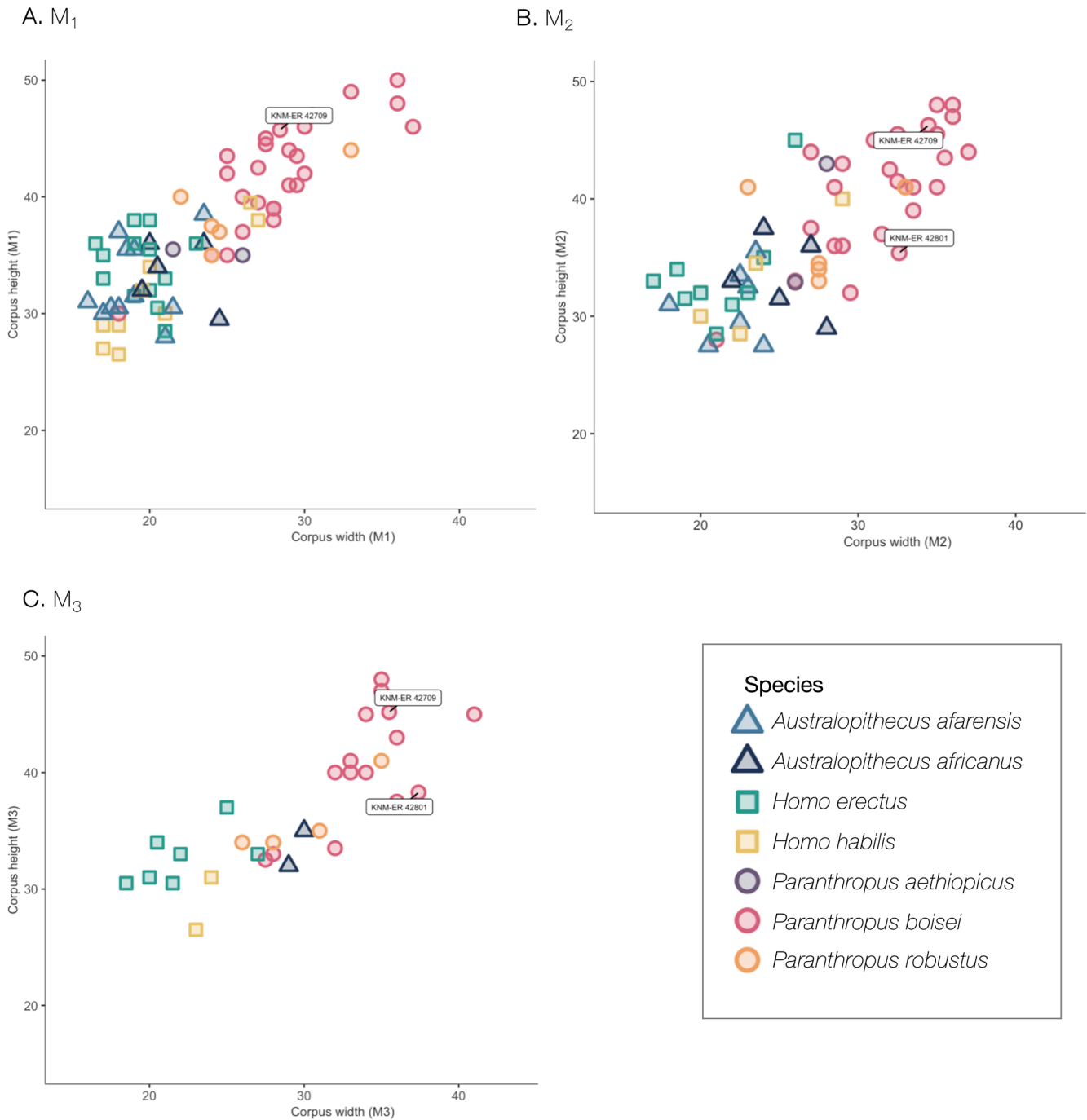


Figure 4. Comparisons of KNM-ER 42709 and KNM-ER 42801 for metric measurements of the mandibular corpus.

sory cusp) (Wood and Constantino 2007). In contrast, distal accessory cusps (C6) in the M₃ of early *Homo* are generally observed in combination with a C7 cusp (Davies et al. 2021).

CONTEXT WITHIN THE *P. BOISEI* MANDIBULAR MORPHOSPACE

In order to contextualize KNM-ER 42709 and KNM-ER 42801 within the shape variability encountered in the *P. boisei* mandibular hypodigm, a geometric morphometric analysis was conducted, and a backtransform morphospace

showing the mandibular corpus profile at M₂ was generated for the first two principal components. Figure 6 illustrates this morphospace, showing a finite distribution of shapes of a transverse section at M₂ of *P. boisei* mandibular corpora along PC1 and PC2 (59.05% of variance explained).

The hypothetical shapes generated by the backtransform of PC1 and PC2 values allow the visualization and description of the diversity in mandibular corpus cross-sections at M₂, and where KNM-ER 42709 and KNM-ER 42801 fall within it. The first principal component (x axis) reflects

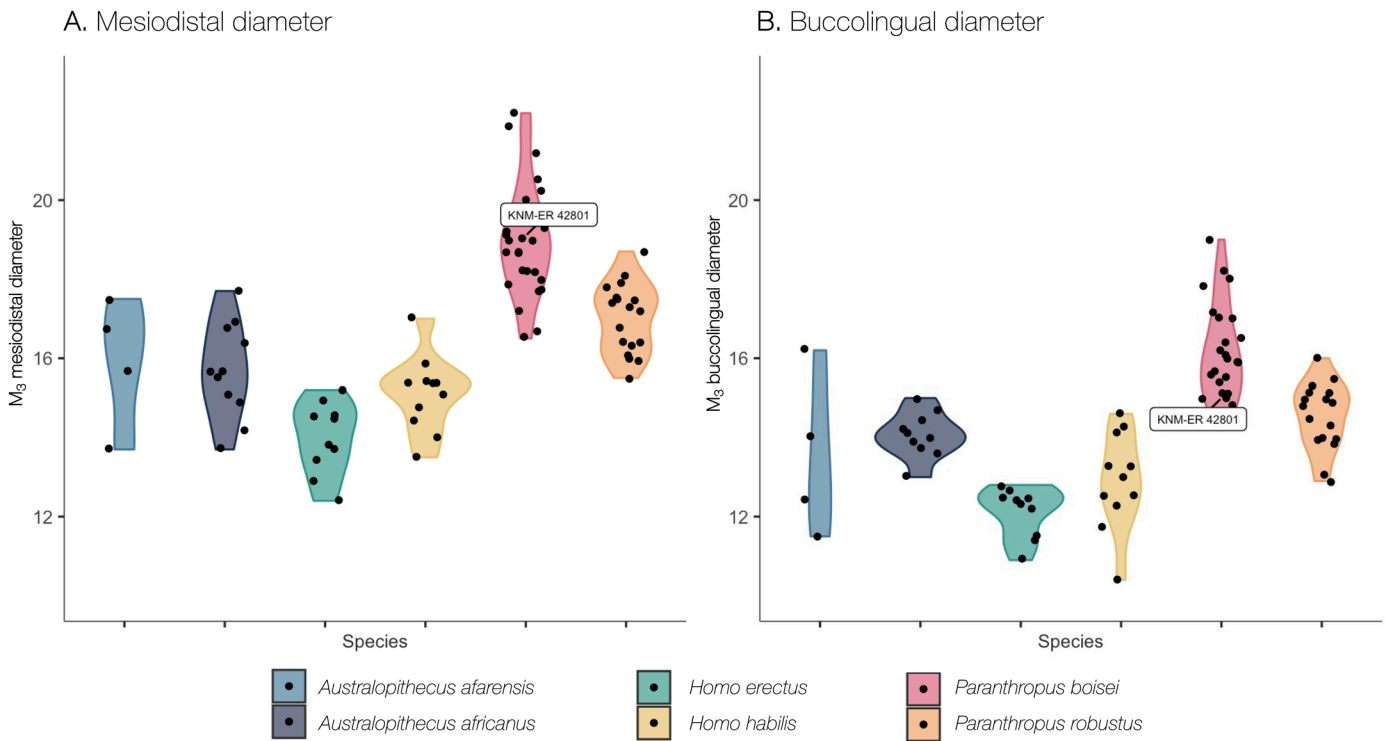


Figure 5. Measurements of buccolingual and mesiodistal diameters of third mandibular molars grouped by species and showing KNM-ER 42801 dimensions. Violin shapes show density distribution.

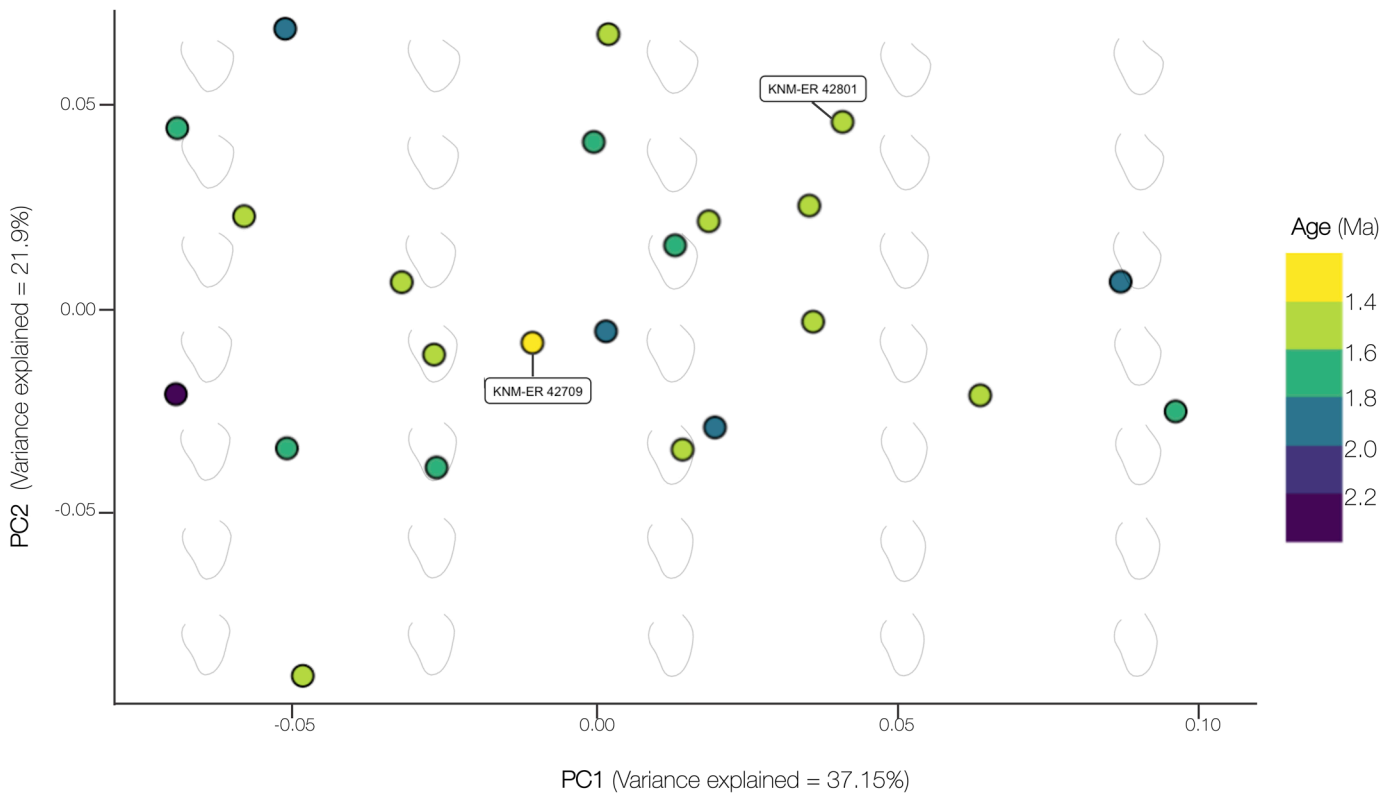


Figure 6. Backtransform morphospace for *P. boisei*, showing distal views of hypothetical mandibular corpus profiles at medial M2. KNM-ER 42709 and KNM-ER 42801 are labelled, and geological age is given in a color scale.

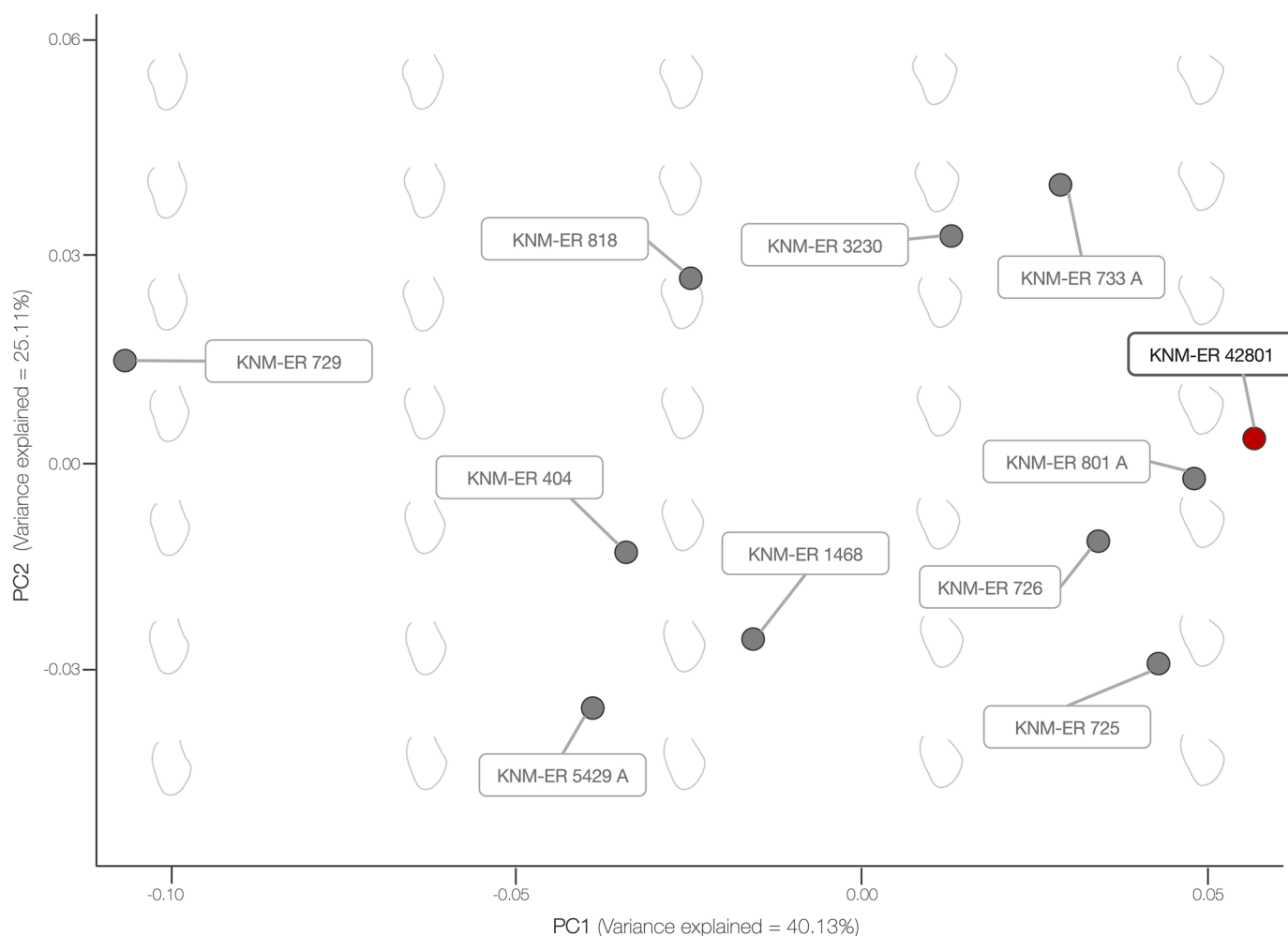


Figure 7. Backtransform morphospace for *P. boisei* samples dated between 1.5 and 1.6 Ma, including KNM-ER 42801 shown in red, and showing distal views of hypothetical mandibular corpus profiles at medial M_2 .

variability in the location of the corpus' widest point, representing the point of maximum projection of the lateral prominence, variability in absolute corpus width, as well as relative width to height (correlated to the Mandibular Robusticity Index, Chamberlain and Wood 1985), and variability in the height of the corpus at which the submandibular fossa is deepest. The second principal component (y axis) reflects variability in the size of the lateral prominence, the buccal projection of the extramolar sulcus, the concavity of the submandibular fossa, and to a lesser extent, the height of the mandibular corpus.

The majority of specimens (82.6 %) fall in the upper left quadrant of the distribution, defining mandibles that are relatively short and wide (i.e., high Robusticity Index), with a pronounced lateral prominence and buccal projection of the extramolar sulcus, and in which the submandibular fossa is relatively shallow and has a relatively low position. Both KNM-ER 42709 and KNM-ER 42801 fall within this morphospace, although the latter is marginal to the distribution. The graph also shows that there is no association between this shape space and geological age of the specimens.

In order to contextualize the variability encountered between 1.5 and 1.6 Ma, corresponding to the estimated age of KNM-ER 42801, a separate PCA was performed using the 11 samples in the *P. boisei* hypodigm dated to this time period. A backtransform morphospace for the first two principal components (65.24% of variance explained) from this analysis was then used to visualize the associated shape changes (Figure 7). The first principal component (x axis) reflects variation in the position and projection of the lateral prominence that defines the buccolingual diameter of the corpus at M_2 and mandibular corpus height. The second principal component (y axis) reflects both differences in the convexity of the lateral protuberance, and the concavity of the submandibular fossa. KNM-ER 42801 falls at the extreme of variation in PC1, displaying the shortest and thickest corpus of this sample set, with the highest lateral protuberance at M_2 .

DISCUSSION

The mandibular morphology of *P. boisei* is characterized by several well-defined and distinctive corpus and dental traits (Wood 1991a). The two fossils described here, KNM-

ER 42709 and KNM-ER 42801, show mandibular and dental character states that are at the core of the *P. boisei* definition, and thus have a clear taxonomic attribution to the species.

Although *P. boisei* has a large chronological range, the majority of the fossils assigned to the species date to between 1.8 and 1.5 Ma and derive from Koobi Fora in the Turkana Basin, with only a handful of *P. boisei* fossils dating to between 1.5 and 1.3 Ma. These include the cranial and dental fossils from Chesowanja, Kenya (KNM-CH 1, KNM-CH 302, and KNM-CH 304) dated to >1.42 Ma (Hooker and Miller 1979), the cranial and mandibular material from Konso, Ethiopia (e.g., KGA 10-525) deriving from a fossiliferous layer dated to between 1.41±0.2 and 1.43±0.2 Ma (Suwa et al. 1997), and the OH 80 postcranial and associated dental remains from Olduvai, Tanzania, dated to 1.338±0.024 Ma (Dominguez-Rodrigo et al. 2013). The geological age of KNM-ER 42709 makes this specimen the last known appearance datum of *P. boisei* in Kenya. It also makes it one of the two youngest mandibular specimens of the hypodigm, the other being the mandible of KGA 10-525.

While younger specimens of *P. boisei* are scarce, a large number of fossils assigned to the taxon are dated to the period between 1.6 and 1.5 Ma, including one-fourth of the *P. boisei* mandibles from Koobi Fora. This temporally and spatially confined group of fossil mandibles shows all the autapomorphic features of the species, but also large variation in the profile shape of the mandibular corpus at M₂, as well as on the buccolingual diameter of the M₂ socket. KNM-ER 42801 falls in geological age within this group. Its morphology marginally increases the variability found in this sample further, including the largest buccolingual M₂ socket of the Koobi Fora sample of this geological age. The morphological heterogeneity of this temporally and geographically synchronous sample highlights the substantial intraspecific variability observed on the whole *P. boisei* mandibular hypodigm, and further confirms previous analyses that suggest the species high variability does not reflect chronological change (Wood et al. 1994), as illustrated in Supplementary Materials Figures S1 and S2.

Part of this variability could be accounted for by the sex composition of the sample, as suggested by several authors (e.g., Conroy and Pontzer 2012). In contrast with extant hominoids (Kimbel 1988), sexual dimorphism in *P. boisei* mandibles has been associated with relatively wider mandibular corpora in males (measured as the Mandibular Robusticity Index, defined as corpus breadth/height at M₁ x100; Chamberlain and Wood 1985). Although the expression of sexual dimorphism in *P. boisei* mandibles is likely to be more complex than just degree of corpus robusticity, on the basis of the latter, KNM-ER 42801, which shows the third widest corpus relative to height, falls among mandibles thought to be male.

Besides increasing the temporal range of *P. boisei* in Kenya, KNM-ER 42709 demonstrates the persistence of the species in Kenya to ca. 1.4 Ma. This has implications for the interpretation of the extirpation of the species in the Turkana Basin, as well as the factors leading to its extinction. A 'C₃ excursion' (i.e., an increase in woody cover) during the

Early to Middle Pleistocene Transition (EMPT, ~1.3–0.7 Ma) in East Africa has been suggested as a significant factor in the extinction of *P. boisei* by Quinn and Lepre (2021). Nonetheless, this 'C₃ excursion' does not occur in a homogenous pattern across the geographical range of *P. boisei*, and C₄ vegetation persisted throughout the EMPT at Koobi Fora (Patterson et al. 2022). The presence of *P. boisei* at younger sections of the Koobi Fora Formation, as demonstrated by KNM-ER 42709, further strengthens the case made by Patterson and colleagues (2022), who suggest the 'C₃ excursion' would not have been a major factor leading to the extinction of the species and makes the survival of the species in East Turkana beyond 1.4 Ma all the more likely.

CONCLUSIONS

The description and analysis of previously unpublished material assigned to *P. boisei* presented here expands the temporal range of this extinct hominin taxon within Kenya and has implications for scenarios related to the disappearance of the species from the regional fossil record. While the factors contributing to the extinction of *P. boisei* remain obscure, the persistence of the species in the Turkana Basin at 1.4 Ma, as shown by KNM-ER 42709, coupled with the presence of C₄ vegetation at Koobi Fora at that time, suggests that the species may have survived locally beyond the onset of the EMPT.

Besides a set of unique characters that distinguish the group from other hominins, *P. boisei* mandibles of similar geological age and close spatial proximity show substantial variation in corpus and dental dimensions. KNM-ER 42801 expands this range of variation in *P. boisei* between 1.5 Ma and 1.6 Ma further. While *P. boisei* remains one of the best represented taxa in the hominin fossil record, the continual expansion of its hypodigm, exemplified by specimens like KNM-ER 42709 and KNM-ER 42801, plays a critical role in enhancing our understanding of the species ecology and evolutionary history.

ACKNOWLEDGEMENTS

We would like to thank the Mexican Council for Science and Technology (CONACYT) and the Cambridge Trust for their support throughout LN's Ph.D., the European Research Council for funding through the IN-AFRICA (ERC 295907) and NG'IPALAJEM (ERC 101020478) Projects, the KFRP, the National Commission for Science, Technology and Innovation (NACOSTI) and National Museums of Kenya (NMK) for permission to conduct research in Kenya (under permits NACOSTI/P/20/3112 to LN and NACOSTI/P/19/513, NACOSTI/P/21/14003, NACOSTI/P/22/22153 to MML), and the support of the staff at NMK, particularly Tom Mukhuyu, Dr. E. Ndiema, and Dr. F.K. Manthi. We also thank the three anonymous reviewers for their useful and constructive comments that improved the manuscript.

DATA AVAILABILITY STATEMENT

3D-landmark coordinate data are available from the corre-

sponding author upon request. All other data are available in the main text or the supplementary materials.



This work is distributed under the terms of a [Creative Commons Attribution-NonCommercial 4.0 Unported License](https://creativecommons.org/licenses/by-nc/4.0/).

REFERENCES

- Bookstein, F.L., 1991. *Morphometric Tools for Landmark Data: Geometry and Biology*. Cambridge University Press, Cambridge. <https://doi.org/10.1017/CBO9780511573064>
- Brown, F.H., Feibel, C.S., 1986. Revision of lithostratigraphic nomenclature in the Koobi Fora region, Kenya. *J. Geol. Soc.* 143, 297–310. <https://doi.org/10.1144/gsjgs.143.2.0297>
- Brown, F.H., Haileab, B., McDougall, I., 2006. Sequence of tuffs between the KBS Tuff and the Chari Tuff in the Turkana Basin, Kenya and Ethiopia. *J. Geol. Soc.* 163, 185–204. <https://doi.org/10.1144/0016-764904-165>
- Chamberlain, A.T., Wood, B.A., 1985. A reappraisal of variation in hominid mandibular corpus dimensions. *Am. J. Phys. Anthropol.* 66, 399–405. <https://doi.org/10.1002/ajpa.1330660408>
- Davies, T.W., Alemseged, Z., Gidna, A., Hublin, J.J., Kimbel, W.H., Kullmer, O., Spoor, F., Zanolli, C., Skinner, M.M., 2021. Accessory cusp expression at the enamel-dentine junction of hominin mandibular molars. *PeerJ* 9, 1–27. <https://doi.org/10.7717/peerj.11415>
- Domínguez-Rodrigo, M., Pickering, T.R., Baquedano, E., Mabulla, A., Mark, D.F., Musiba, C., Bunn, H.T., Uribelarra, D., Smith, V., Diez-Martin, F., Pérez-González, A., Sánchez, P., Santonja, M., Barboni, D., Gidna, A., Ashley, G., Yravedra, J., Heaton, J.L., Arriaza, M.C., 2013. First partial skeleton of a 1.34-million-year-old *Paranthropus boisei* from Bed II, Olduvai Gorge, Tanzania. *PLoS One* 8, e80347. <https://doi.org/10.1371/journal.pone.0080347>
- Gathogo, P.N., Brown, F.H., 2006. Stratigraphy of the Koobi Fora Formation (Pliocene and Pleistocene) in the Ileret region of northern Kenya. *J. African Earth Sci.* 45, 369–390. <https://doi.org/10.1016/j.jafrearsci.2006.03.006>
- Gunz, P., Mitteroecker, P., 2013. Semilandmarks: a method for quantifying curves and surfaces. *Hystrix* 24, 103–109. <https://doi.org/10.4404/hystrix-24.1-6292>
- Harris, J.M., Leakey, M.G., Brown, F.H., 2006. A brief history of research at Koobi Fora, Northern Kenya. *Ethnohistory*, 53, 35–69. <https://doi.org/10.1215/00141801-53-1-35>
- Hooker, P.J., Miller, J.A., 1979. K-Ar dating of the Pleistocene fossil hominid site at Chesowanja, North Kenya. *Nature* 282, 710–712. <https://doi.org/10.1038/282710a0>
- Klein, R., 1988. The causes of “robust” australopithecine extinction. In: Grine, F. (Ed.), *Evolutionary History of the “Robust” Australopithecines*. Aldine De Gruyter, New York, pp. 499–505. <https://doi.org/10.4324/9780203792667>
- Klingenberg, C.P., 2010. Evolution and development of shape: integrating quantitative approaches. *Nat. Rev. Genet.* 11, 623–635. <https://doi.org/10.1038/nrg2829>
- Kullmer, O., Sandrock, O., Abel, R., Schrenk, F., Bromage, T. G., Juwayeyi, Y. M., 1999. The first *Paranthropus* from the Malawi Rift. *J. Hum. Evol.* 37, 121–127. <https://doi.org/10.1006/jhev.1999.0308>
- Leakey, L.S.B., Leakey, M.D., 1964. Recent discoveries of fossil hominids in Tanganyika: at Olduvai and near lake Natron. *Nature* 202, 5–7. <https://doi.org/10.1038/202005a0>
- Leakey, M.G., Spoor, F., Dean, M.C., Feibel, C.S., Antón, S.C., Kiarie, C., Leakey, L.N., 2012. New fossils from Koobi Fora in northern Kenya confirm taxonomic diversity in early *Homo*. *Nature* 488, 201–204. <https://doi.org/10.1038/nature11322>
- Leakey, R.E., Walker, A., 1976. *Australopithecus*, *Homo erectus* and the single species hypothesis. *Nature* 261, 572–574. <https://doi.org/10.1038/261572a0>
- McDougall, I., Brown, F.H., 2006. Precise ⁴⁰Ar/³⁹Ar geochronology for the upper Koobi Fora Formation, Turkana Basin, northern Kenya. *J. Geol. Soc.* 163, 205–220. <https://doi.org/10.1144/0016-764904-166>
- Patterson, D.B., Braun, D.R., Behrensmeier, A.K., Lehmann, S.B., Merritt, S.R., Reeves, J.S., Wood, B.A., Bobe, R., 2017. Landscape scale heterogeneity in the East Turkana ecosystem during the Okote Member (1.56–1.38 Ma). *J. Hum. Evol.* 112, 148–161. <https://doi.org/10.1016/j.jhevol.2017.06.007>
- Patterson, D.B., Du, A., Faith, J.T., Rowan, J., Uno, K., Behrensmeier, A.K., Braun, D.R., Wood, B.A., 2022. Did vegetation change drive the extinction of *Paranthropus boisei*? *J. Hum. Evol.* 173, 103154. <https://doi.org/10.1016/j.jhevol.2022.103154>
- Quinn, R.L., Lepre, C.J., 2021. Contracting eastern African C₄ grasslands during the extinction of *Paranthropus boisei*. *Sci. Rep.* 11, 1–10. <https://doi.org/10.1038/s41598-021-86642-z>
- Quinn, R.L., Lepre, C.J., Feibel, C.S., Wright, J.D., Mortlock, R.A., Harmand, S., Brugal, J.P., Roche, H., 2013. Pedogenic carbonate stable isotopic evidence for wooded habitat preference of early Pleistocene tool makers in the Turkana Basin. *J. Hum. Evol.* 65, 65–78. <https://doi.org/10.1016/j.jhevol.2013.04.002>
- Schlager, S., 2017. Morpho and Rvcg – Shape Analysis in R. In: Zheng, G., Li, S., Székely, G. (Eds.), *Statistical Shape and Deformation Analysis*. Academic Press, New York, pp. 217–256. <https://doi.org/10.1016/C2015-0-06799-5>
- Spoor, F., Leakey, M.G., Gathogo, P.N., Brown, F.H., Antón, S.C., McDougall, I., Kiarie, C., Manthi, F.K., Leakey, L.N., 2007. Implications of new early *Homo* fossils from Ileret, east of Lake Turkana, Kenya. *Nature* 448, 688–691. <https://doi.org/10.1038/nature05986>
- Suwa, G., Asfaw, B., Beyene, Y., White, T. D., Katoh, S., Nagaoka, S., Nakaya, H., Uzawa, K., Renne, P., Wolde-Gabriel, G., 1997. The first skull of *Australopithecus boisei*. *Nature* 389, 489–492. <https://doi.org/10.1038/39037>
- Ungar, P.S., Grine, F.E., Teaford, M.F., 2008. Dental microwear and diet of the Plio-Pleistocene hominin

- Paranthropus boisei*. PLoS One 3, e2044. <https://doi.org/10.1371/journal.pone.0002044>
- White, T.D., 1988. The comparative biology of “robust” *Australopithecus*: clues from context. In: Grine, F.E. (Ed.), *Evolutionary History of the “Robust” Australopithecines*. Routledge, New York, pp. 449–483. <https://doi.org/10.4324/9780203792667>
- Wood, B.A., 1991a. Koobi Fora Research Project, Volume 4: Hominid Cranial Remains. Oxford University Press, Oxford.
- Wood, B.A., 1991b. A palaeontological model for determining the limits of early hominid taxonomic variability. *Palaeontol. Afr.* 28, 71–77.
- Wood, B.A., Abbott, S.A., 1983. Analysis of the dental morphology of Plio-Pleistocene hominids. I. Mandibular molars: crown area measurements and morphological traits. *J. Anat.* 136, 197–219.
- Wood, P.B., Constantino, P., 2007. *Paranthropus boisei*: Fifty years of evidence and analysis. *Am. J. Phys. Anthropol.* 134, 106–132. <https://doi.org/10.1002/ajpa.20732>
- Wood, B.A., Patterson, D.B., 2020. *Paranthropus* through the looking glass. *Proc. Nat. Acad. Sci.* 117, 23202–23204. <https://doi.org/10.1073/pnas.2016445117>
- Wood, B.A., Strait, D., 2004. Patterns of resource use in early *Homo* and *Paranthropus*. *J. Hum. Evol.* 46, 119–162. <https://doi.org/10.1016/j.jhevol.2003.11.004>
- Wood, B.A., Abbott, S.A., Uytterschaut, H., 1988. Analysis of the dental morphology of Plio-Pleistocene hominids IV. Mandibular postcanine root morphology. *J. Anat.* 156, 107–139.
- Wood, B.A., Wood, C., Konigsberg, L., 1994. *Paranthropus boisei*: an example of evolutionary stasis? *Am. J. Phys. Anthropol.* 95, 117–136. <https://doi.org/10.1002/ajpa.1330950202>

Supplement 1: New Additions to the *Paranthropus boisei* Mandibular Hypodigm from Koobi Fora, Kenya

LUCÍA NADAL*

*Leverhulme Centre for Human Evolutionary Studies, Department of Archaeology, University of Cambridge, Cambridge, UNITED KINGDOM;
and, Turkana Basin Institute, Nairobi, KENYA; ln340@cam.ac.uk*

LOUISE LEAKEY

*Turkana Basin Institute, Nairobi, KENYA; and, Department of Anthropology, Stony Brook University, Stony Brook, USA;
louise.leakey@stonybrook.edu*

MEAVE LEAKEY

*Turkana Basin Institute, Nairobi, KENYA; and, Department of Anthropology, Stony Brook University, Stony Brook, USA;
meave.leakey@stonybrook.edu*

MARTA MIRAZÓN LAHR

*Leverhulme Centre for Human Evolutionary Studies, Department of Archaeology, University of Cambridge, Cambridge, UNITED KINGDOM;
and, Turkana Basin Institute, Nairobi, KENYA; mbml1@cam.ac.uk*

SUPPLEMENT 1

This file includes: Supplementary Figures S1–S2 and Tables S1–S6.

**TABLE S1. MANDIBULAR AND DENTAL MEASUREMENTS
OF KNM-ER 42709 and KNM-ER 42801.**

Measurement	KNM-ER 42709	KNM-ER 42801
Chin height	43.8	–
Symphyseal depth (Max)	27.34	–
Symphyseal depth (STT)	27.34	–
Symphyseal depth (ITT)	26.88	–
Corpus height at P4	49.06 (L)	–
Corpus width at P4	27.6 (L)	–
Corpus height at M1	45.74 (L)	–
Corpus width at M1	28.41 (L)	–
Corpus height at M2	46.26 (L)	35.41 (R)
Corpus width at M2	34.46 (L)	32.64 (R)
Corpus height at M3	45.19 (L)	38.29 (R)
Corpus width at M3	35.5 (L)	37.47 (R)
Height of mental foramen (B)	27.82 (L)	–
Height of mental foramen (A1)	18.04 (L)	–
I1-I2 alveolar length	10.29 (L)	–
P3-P4 alveolar length	25.02 (L)	–
M1-M3 alveolar length	55.35 (L)	–

*All measurements shown in mm and taken as described by Wood (1991a) using a digital calliper and rounded to the nearest 0.01 mm.

TABLE S2. COMPARATIVE FOSSIL MEASUREMENTS FOR M₁ CORPUS HEIGHT AND M₁ CORPUS WIDTH COMPILED FROM WOOD (1991a).

Fossil ID	Taxon	M₁ corpus height (mm)	M₁ corpus width (mm)
AL 145-35	<i>Australopithecus afarensis</i>	28	21
AL 198-1	<i>Australopithecus afarensis</i>	31	16
AL 207-13	<i>Australopithecus afarensis</i>	30.5	18
AL 266-1	<i>Australopithecus afarensis</i>	30.5	21.5
AL 277-1	<i>Australopithecus afarensis</i>	37	18
AL 288-1i	<i>Australopithecus afarensis</i>	30	17
AL 333w-1a+b	<i>Australopithecus afarensis</i>	35.5	19
AL 333w-12	<i>Australopithecus afarensis</i>	30.5	17.5
AL 333w-32+60	<i>Australopithecus afarensis</i>	38.5	23.5
AL 400-1a	<i>Australopithecus afarensis</i>	35.5	18.5
LH 4	<i>Australopithecus afarensis</i>	31.5	19
MLD 18	<i>Australopithecus africanus</i>	34	20.5
MLD 34	<i>Australopithecus africanus</i>	32	19.5
MLD 40	<i>Australopithecus africanus</i>	36	23.5
Sts 36	<i>Australopithecus africanus</i>	36	20
Sts 52	<i>Australopithecus africanus</i>	29.5	24.5
OH 22	<i>Homo erectus</i>	28.5	21
OH 23	<i>Homo erectus</i>	33	21
KNM-ER 992	<i>Homo erectus</i>	32	20
KNM-ER 730	<i>Homo erectus</i>	31.5	19
KNM-BK 67	<i>Homo erectus</i>	33	17
KNM-BK 8518	<i>Homo erectus</i>	30.5	20.5
Sangiran 1b	<i>Homo erectus</i>	36	16.5
Sangiran 5	<i>Homo erectus</i>	38	20
Sangiran 8	<i>Homo erectus</i>	35.5	20
Sangiran 9	<i>Homo erectus</i>	36	23
Tighenif 1	<i>Homo erectus</i>	36	19
Tighenif 2	<i>Homo erectus</i>	35	17
Tighenif 3	<i>Homo erectus</i>	38	19
OH 13	<i>Homo habilis</i>	26.5	18
OH 37	<i>Homo habilis</i>	32	19.5
KNM-ER 1805	<i>Homo habilis</i>	30	21
KNM-ER 1483	<i>Homo habilis</i>	39.5	26.5
KNM-ER 1501	<i>Homo habilis</i>	29	17
KNM-ER 1502	<i>Homo habilis</i>	27	17
KNM-ER 1801	<i>Homo habilis</i>	34	20
KNM-ER 819	<i>Homo habilis</i>	38	27
KNM-ER 817	<i>Homo habilis</i>	29	18

OMO L860-2	<i>Paranthropus aethiopicus</i>	35.5	21.5
OMO 18.18	<i>Paranthropus aethiopicus</i>	35	26
SK 6	<i>Paranthropus robustus</i>	37.5	24
SK 12	<i>Paranthropus robustus</i>	44	33
SK 23	<i>Paranthropus robustus</i>	37	24.5
SK 34	<i>Paranthropus robustus</i>	40	22
TM 1517	<i>Paranthropus robustus</i>	35	24
KNM-ER 403	<i>Paranthropus boisei</i>	47	30.5
KNM-ER 725	<i>Paranthropus boisei</i>	41	29.5
KNM-ER 726	<i>Paranthropus boisei</i>	46	30
KNM-ER 727	<i>Paranthropus boisei</i>	35	24
KNM-ER 728	<i>Paranthropus boisei</i>	37	26
KNM-ER 729	<i>Paranthropus boisei</i>	44.5	27.5
KNM-ER 733	<i>Paranthropus boisei</i>	39.5	27
KNM-ER 801A	<i>Paranthropus boisei</i>	43.5	29.5
KNM-ER 805A	<i>Paranthropus boisei</i>	41	29
KNM-ER 810A	<i>Paranthropus boisei</i>	40	26
KNM-ER 818	<i>Paranthropus boisei</i>	50	36
KNM-ER 1468	<i>Paranthropus boisei</i>	48	36
KNM-ER 1469	<i>Paranthropus boisei</i>	46	37
KNM-ER 1803	<i>Paranthropus boisei</i>	42	25
KNM-ER 1806	<i>Paranthropus boisei</i>	45	27.5
KNM-ER 3229	<i>Paranthropus boisei</i>	39	28
KNM-ER 3230	<i>Paranthropus boisei</i>	42	30
KNM-ER 3729	<i>Paranthropus boisei</i>	38	28
KNM-ER 3731	<i>Paranthropus boisei</i>	30	18
KNM-ER 5877	<i>Paranthropus boisei</i>	44	29
KNM-ER 15930	<i>Paranthropus boisei</i>	35	25
KNM-ER 16841	<i>Paranthropus boisei</i>	42.5	27
OMO L7A-125	<i>Paranthropus boisei</i>	49	33
OMO L74A-21	<i>Paranthropus boisei</i>	43.5	25
Peninj 1	<i>Paranthropus boisei</i>	39	28

TABLE S3. COMPARATIVE FOSSIL MEASUREMENTS FOR M₂ CORPUS HEIGHT AND M₂ CORPUS WIDTH COMPILED FROM WOOD (1991a).

Fossil ID	Taxon	M ₂ corpus height (mm)	M ₂ corpus width (mm)
AL 188-1	<i>Australopithecus afarensis</i>	33.5	22.5
AL 198-1	<i>Australopithecus afarensis</i>	31	18
AL 207-13	<i>Australopithecus afarensis</i>	27.5	20.5
AL 266-1	<i>Australopithecus afarensis</i>	27.5	24
AL 333w-1a+b	<i>Australopithecus afarensis</i>	32.5	23
AL 333w-32+60	<i>Australopithecus afarensis</i>	35.5	23.5
LH 4	<i>Australopithecus afarensis</i>	29.5	22.5
MLD 18	<i>Australopithecus africanus</i>	31.5	25
MLD 34	<i>Australopithecus africanus</i>	33	22
MLD 40	<i>Australopithecus africanus</i>	36	27
Sts 36	<i>Australopithecus africanus</i>	37.5	24
Sts 52	<i>Australopithecus africanus</i>	29	28
KNM-ER 1501	<i>Homo habilis</i>	30	20
OH 37	<i>Homo habilis</i>	34.5	23.5
KNM-ER 819	<i>Homo habilis</i>	40	29
OH 13	<i>Homo habilis</i>	28.5	22.5
OH 22	<i>Homo erectus</i>	28.5	21
OH 23	<i>Homo erectus</i>	32	20
KNM-ER 992	<i>Homo erectus</i>	35	24
KNM-ER 730	<i>Homo erectus</i>	31.5	19
KNM-BK 67	<i>Homo erectus</i>	34	18.5
KNM-BK 8518	<i>Homo erectus</i>	31	22
Sangiran 1b	<i>Homo erectus</i>	33	17
Sangiran 6	<i>Homo erectus</i>	45	26
Sangiran 9	<i>Homo erectus</i>	32	23
OMO 18.18	<i>Paranthropus aethiopicus</i>	33	26
OMO 57.41	<i>Paranthropus aethiopicus</i>	43	28
SK 6	<i>Paranthropus robustus</i>	33	27.5
SK 12	<i>Paranthropus robustus</i>	41	33
SK 23	<i>Paranthropus robustus</i>	34.5	27.5
SK 34	<i>Paranthropus robustus</i>	41	23
TM 1517	<i>Paranthropus robustus</i>	34	27.5
KNM-ER 403	<i>Paranthropus boisei</i>	45.5	32.5
KNM-ER 404	<i>Paranthropus boisei</i>	45.5	35
KNM-ER 725	<i>Paranthropus boisei</i>	41.5	32.5
KNM-ER 726	<i>Paranthropus boisei</i>	45	31
KNM-ER 727	<i>Paranthropus boisei</i>	33	26
KNM-ER 728	<i>Paranthropus boisei</i>	37.5	27

KNM-ER 729	<i>Paranthropus boisei</i>	43	29
KNM-ER 733	<i>Paranthropus boisei</i>	36	29
KNM-ER 801A	<i>Paranthropus boisei</i>	42.5	32
KNM-ER 805A	<i>Paranthropus boisei</i>	39	33.5
KNM-ER 810A	<i>Paranthropus boisei</i>	41	33.5
KNM-ER 818	<i>Paranthropus boisei</i>	48	36
KNM-ER 1468	<i>Paranthropus boisei</i>	47	36
KNM-ER 1469	<i>Paranthropus boisei</i>	44	37
KNM-ER 1806	<i>Paranthropus boisei</i>	41	28.5
KNM-ER 3229	<i>Paranthropus boisei</i>	41	33
KNM-ER 3230	<i>Paranthropus boisei</i>	41	35
KNM-ER 3729	<i>Paranthropus boisei</i>	36	28.5
KNM-ER 3731	<i>Paranthropus boisei</i>	28	21
KNM-ER 5877	<i>Paranthropus boisei</i>	43.5	35.5
KNM-ER 15930	<i>Paranthropus boisei</i>	32	29.5
KNM-ER 16841	<i>Paranthropus boisei</i>	44	27
OMO L7A-125	<i>Paranthropus boisei</i>	48	35
Peninj 1	<i>Paranthropus boisei</i>	37	31.5

TABLE S4. COMPARATIVE FOSSIL MEASUREMENTS FOR M₃ CORPUS HEIGHT AND M₃ CORPUS WIDTH COMPILED FROM WOOD (1991a).

Fossil ID	Taxon	M₃ corpus height (mm)	M₃ corpus width (mm)
MLD 18	<i>Australopithecus africanus</i>	32	29
MLD 40	<i>Australopithecus africanus</i>	35	30
OH 13	<i>Homo habilis</i>	26.5	23
OH 37	<i>Homo habilis</i>	31	24
KNM-ER 730	<i>Homo erectus</i>	30.5	18.5
KNM-ER 992	<i>Homo erectus</i>	37	25
OH 22	<i>Homo erectus</i>	33	22
KNM-BK 67	<i>Homo erectus</i>	34	20.5
KNM-BK 8518	<i>Homo erectus</i>	30.5	21.5
Sangiran 1b	<i>Homo erectus</i>	31	20
Sangiran 9	<i>Homo erectus</i>	33	27
SK 12	<i>Paranthropus robustus</i>	41	35
SK 23	<i>Paranthropus robustus</i>	34	28
SK 34	<i>Paranthropus robustus</i>	35	31
TM 1517	<i>Paranthropus robustus</i>	34	26
KNM-ER 403	<i>Paranthropus boisei</i>	45	34
KNM-ER 725	<i>Paranthropus boisei</i>	37.5	36
KNM-ER 726	<i>Paranthropus boisei</i>	41	33
KNM-ER 729	<i>Paranthropus boisei</i>	43	36
KNM-ER 801A	<i>Paranthropus boisei</i>	40	33
KNM-ER 1468	<i>Paranthropus boisei</i>	47	35
KNM-ER 1469	<i>Paranthropus boisei</i>	45	41
KNM-ER 3229	<i>Paranthropus boisei</i>	40	34
KNM-ER 3729	<i>Paranthropus boisei</i>	33	28
KNM-ER 15930	<i>Paranthropus boisei</i>	32.5	27.5
KNM-ER 16841	<i>Paranthropus boisei</i>	40	32
OMO L7A-125	<i>Paranthropus boisei</i>	48	35
Peninj 1	<i>Paranthropus boisei</i>	33.5	32

TABLE S5. COMPARATIVE FOSSIL SAMPLE FOR M₃ CROWN DIAMETERS
COMPILED FROM WOOD (1991a).

Fossil ID	Taxon	M ₃ mesiodistal diameter (mm)	M ₃ buccolingual diameter (mm)
OMO L795-1	<i>Australopithecus afarensis</i>	175	162
OMO L9-11	<i>Australopithecus afarensis</i>	157	140
OMO L28-30	<i>Australopithecus afarensis</i>	167	124
OMO L2-89	<i>Australopithecus afarensis</i>	137	115
MLD 4	<i>Australopithecus africanus</i>	—	142
MLD 18	<i>Australopithecus africanus</i>	142	139
MLD 19	<i>Australopithecus africanus</i>	151	136
TM 1518	<i>Australopithecus africanus</i>	168	150
TM 1519	<i>Australopithecus africanus</i>	157	140
TM 1520	<i>Australopithecus africanus</i>	169	141
Sts 3	<i>Australopithecus africanus</i>	157	—
Sts 7	<i>Australopithecus africanus</i>	164	144
Sts 41	<i>Australopithecus africanus</i>	149	—
Sts 52b	<i>Australopithecus africanus</i>	137	130
Sts 55b	<i>Australopithecus africanus</i>	155	137
Stw/H 14	<i>Australopithecus africanus</i>	177	147
OMO 75-14a	<i>Homo habilis</i>	151	141
OMO 75s-16	<i>Homo habilis</i>	140	117
OH 4	<i>Homo habilis</i>	154	130
OH 13	<i>Homo habilis</i>	148	123
OH 16	<i>Homo habilis</i>	159	143
OH 27	<i>Homo habilis</i>	154	133
KNM-ER 3953	<i>Homo habilis</i>	154	125
KNM-ER 2601	<i>Homo habilis</i>	135	104
KNM-ER 1801	<i>Homo habilis</i>	170	146
KNM-ER 1480	<i>Homo habilis</i>	154	125
KNM-ER 1462	<i>Homo habilis</i>	144	133
KNM-ER 730	<i>Homo erectus</i>	137	115
KNM-ER 806A	<i>Homo erectus</i>	149	124
KNM-ER 992B	<i>Homo erectus</i>	134	123
KNM-ER 1812C	<i>Homo erectus</i>	145	125
KNM-BK 67	<i>Homo erectus</i>	129	114
SK 15	<i>Homo erectus</i>	146	122
Sangiran 1b	<i>Homo erectus</i>	145	125
Sangiran 8	<i>Homo erectus</i>	152	128
Sangiran 9	<i>Homo erectus</i>	138	127
Sangiran 21	<i>Homo erectus</i>	124	109
TM 1517	<i>Paranthropus robustus</i>	164	143
TM 1600	<i>Paranthropus robustus</i>	161	149
SK 6	<i>Paranthropus robustus</i>	187	155
SK 12	<i>Paranthropus robustus</i>	173	153
SK 23	<i>Paranthropus robustus</i>	168	131
SK 34	<i>Paranthropus robustus</i>	181	160
SK 75	<i>Paranthropus robustus</i>	175	150

SK 81	<i>Paranthropus robustus</i>	174	148
SK 840	<i>Paranthropus robustus</i>	164	129
SK 841b	<i>Paranthropus robustus</i>	159	138
SK 843	<i>Paranthropus robustus</i>	175	151
SK 844	<i>Paranthropus robustus</i>	160	140
SK 858	<i>Paranthropus robustus</i>	175	—
SK 880	<i>Paranthropus robustus</i>	179	145
SK 885	<i>Paranthropus robustus</i>	155	140
SK 1586	<i>Paranthropus robustus</i>	163	151
SKX 5002	<i>Paranthropus robustus</i>	178	139
SKX 5014	<i>Paranthropus robustus</i>	172	150
KNM-ER 729	<i>Paranthropus boisei</i>	212	190
KNM-ER 733A	<i>Paranthropus boisei</i>	190	—
KNM-ER 801A	<i>Paranthropus boisei</i>	192	160
KNM-ER 802F	<i>Paranthropus boisei</i>	187	164
KNM-ER 810B	<i>Paranthropus boisei</i>	177	157
KNM-ER 818	<i>Paranthropus boisei</i>	219	182
KNM-ER 1467	<i>Paranthropus boisei</i>	187	154
KNM-ER 1509A	<i>Paranthropus boisei</i>	198	159
KNM-ER 1819	<i>Paranthropus boisei</i>	222	—
KNM-ER 3230	<i>Paranthropus boisei</i>	205	165
KNM-ER 15930	<i>Paranthropus boisei</i>	182	150
KNM-ER 15940	<i>Paranthropus boisei</i>	180	155
KNM-ER 15950	<i>Paranthropus boisei</i>	200	170
KNM-WT 17396	<i>Paranthropus boisei</i>	190	170
OMO L7A-125	<i>Paranthropus boisei</i>	182	148
OMO L338x-39	<i>Paranthropus boisei</i>	194	151
OMO L398-630	<i>Paranthropus boisei</i>	177	147
OMO L628-2	<i>Paranthropus boisei</i>	190	178
OMO L628-3	<i>Paranthropus boisei</i>	187	162
OMO 33-9	<i>Paranthropus boisei</i>	193	151
OMO 33-65	<i>Paranthropus boisei</i>	165	—
OMO 136-1	<i>Paranthropus boisei</i>	179	156
OMO 136-2	<i>Paranthropus boisei</i>	167	146
OMO F22-1b	<i>Paranthropus boisei</i>	202	180
OMO F203-1	<i>Paranthropus boisei</i>	172	159
OMO L398-847	<i>Paranthropus boisei</i>	—	172
PENINJ	<i>Paranthropus boisei</i>	182	161

TABLE S6. EXPECTED EXPRESSION ACROSS TAXA OF MANDIBULAR AND DENTAL TRAITS PRESERVED IN KNM-ER 42709 and KNM-ER 42801.

	<i>P. boisei</i>	early <i>Homo</i>	<i>P. aethiopicus</i>	<i>P. robustus</i>
1. Lingual aspect of the mandibular corpus	Large and well-defined superior and inferior transverse tori. In most cases, the inferior torus is larger than the superior one.	Some degree of variability is present and while a single torus mandibularis can be seen on the lingual aspect of the corpus of some specimens, for the most part this is absent.	Large and well-defined superior and inferior transverse tori. In most cases, the inferior torus is larger than the superior one.	Large and well-defined superior and inferior transverse tori. In most cases, the inferior torus is larger than the superior one.
2. Buccal aspect of the mandibular corpus	Substantial buttressing and a notable lateral corpus prominence are present usually below M ₁ -M ₂ .	A lateral prominence is present usually below the M ₂	A lateral corpus prominence is present usually below M ₁ -M ₂ .	Substantial buttressing and a notable lateral corpus prominence are present usually below M ₁ -M ₂ .
3. Extramolar sulcus	A characteristically wide and deep extramolar sulcus is present across the sample.	While some degree of variability in the width of the extramolar sulcus is observed across this sample, for the most part the extramolar sulcus is narrow.	A wide extramolar sulcus can be observed across the species' mandibular hypodigm.	A wide extramolar sulcus can be observed across the species' mandibular hypodigm.
5. P ₄ root morphology	Two mesiodistally flattened roots.	Tomes' root and two canals.	Two mesiodistally flattened roots.	Two mesiodistally flattened roots.
6. P ₃ root morphology	Two mesiodistally flattened roots.	Both Tomes' root and single root are observed across the hypodigm.	Two mesiodistally flattened roots.	Tomes' root and two canals.
7. Accessory cusps in M ₃ crown	Presence of distal cusps (C ₆), and absence of lingual cusps (C ₇). C ₇ present in rare cases and always in combination with C ₆ .	Accessory cusps are present either in the form of only a lingual cusp (C ₇), or a C ₇ accompanied by a C ₆ .	Presence of distal cusps (C ₆), and absence of lingual cusps (C ₇). C ₇ present in rare cases and always in combination with C ₆ .	Presence of distal cusps (C ₆), and absence of lingual cusps (C ₇). C ₇ present in rare cases and always in combination with C ₆ .

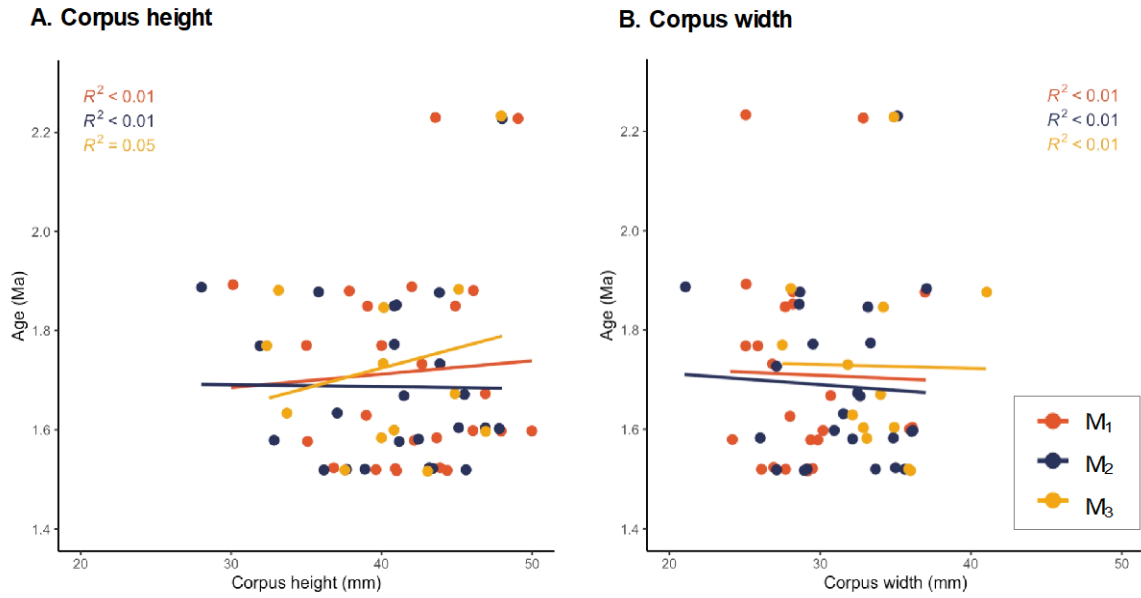


Figure S1. Corpus dimensions (i.e., width and height), and geological age of the *P. boisei* comparative sample used in this study. Linear regressions and associated R-squared values are shown for M_1 , M_2 and M_3 . Metric measurements were compiled from Wood (1991a), and age values averaged from Wood and Constantino (2007).

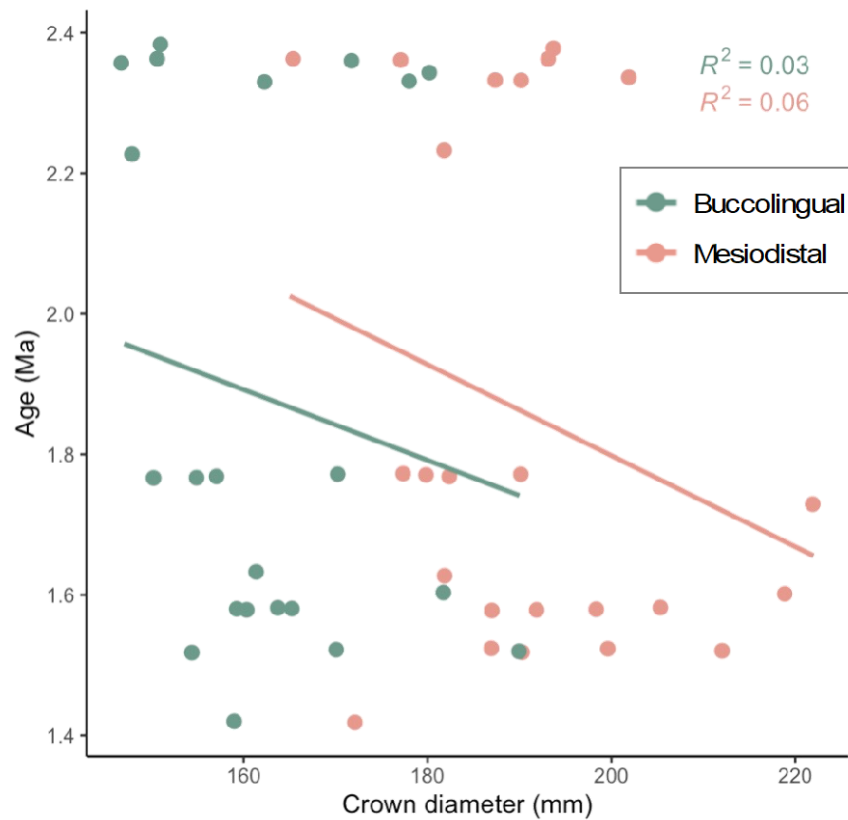


Figure S2. M_3 crown diameters and geological age of the *P. boisei* comparative sample used in this study. Linear regressions and associated R-squared values are shown for buccolingual and mesiodistal diameters. Metric measurements were compiled from Wood (1991a), and age values averaged from Wood and Constantino (2007).